Sensitivity of seismic waves to structure: Wide-angle broad-band sensitivity packets

Luděk Klimeš

Department of Geophysics
Faculty of Mathematics and Physics
Charles University in Prague

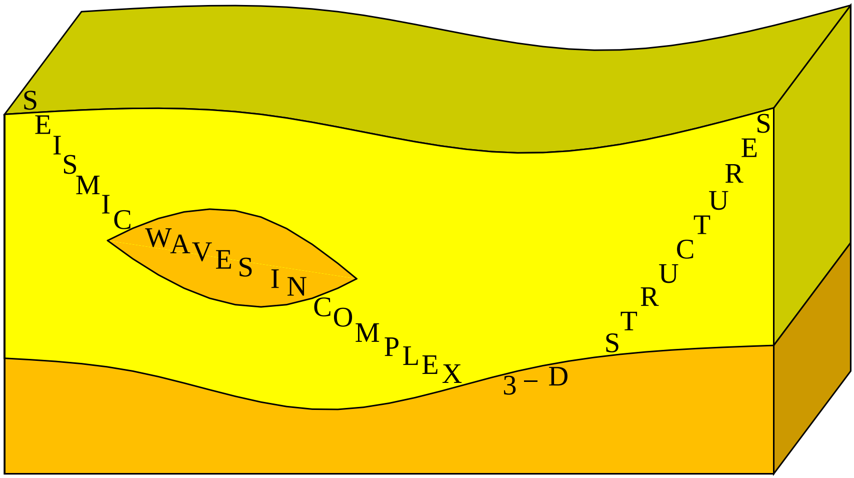

http://sw3d.cz

Sensitivity of seismic waves to structure: Wide-angle broad-band sensitivity packets

Luděk Klimeš

We study how the perturbations of a generally heterogeneous isotropic or anisotropic structure manifest themselves in the wave field, and which perturbations can be detected within a limited aperture and a limited frequency band.

This study represents a generalization of the narrow-band Gaussian sensitivity packets (Klimeš, 2012) to the broad-band sensitivity packets.

We shall concentrate especially on the differences between the Gaussian sensitivity packets and the broad-band sensitivity packets.

Sensitivity of seismic waves to structure: Wide-angle broad-band sensitivity packets

Luděk Klimeš

Outline

Gabor representation of medium perturbations
Applied approximations
Initial slowness vector of the Gaussian sensitivity beam
Inverse frequencies ϖ^0 for different structural wavenumber vectors k_i^α
Initial slowness vector of the broad-band sensitivity beam
Paraxial approximation of the sensitivity beam
Evolution equations of the sensitivity beam
Paraxial approximation of the sensitivity packet
Evolution equations of the sensitivity packet
Illustrations of the broad-band sensitivity packets
Conclusions
References (online at "http://sw3d.cz")
Acknowledgements

Gabor representation of medium perturbations

We assume a smoothly varying heterogeneous generally anisotropic elastic background medium.

We consider arbitrarily heterogeneous infinitesimally small perturbations $\delta c_{ijkl}(\mathbf{x})$ and $\delta\varrho(\mathbf{x})$ of elastic moduli $c_{ijkl}(\mathbf{x})$ and density $\varrho(\mathbf{x})$.

We decompose the perturbations into Gabor functions $g^\alpha(\mathbf{x})$ indexed here by Ω:

$$\delta c_{ijkl}(\mathbf{x}) = \sum_\alpha c^\alpha_{ijkl}\, g^\alpha(\mathbf{x}) \quad , \qquad \delta\varrho(\mathbf{x}) = \sum_\alpha \varrho^\alpha\, g^\alpha(\mathbf{x}) \quad ,$$

$$g^\alpha(\mathbf{x}) = \exp[\mathrm{i}\,\mathbf{k}^{\alpha\,\mathrm{T}}(\mathbf{x}-\mathbf{x}^\alpha) - \tfrac{1}{2}(\mathbf{x}-\mathbf{x}^\alpha)^{\mathrm{T}}\mathbf{K}^\alpha(\mathbf{x}-\mathbf{x}^\alpha)] \quad .$$

Gabor functions $g^\alpha(\mathbf{x})$ are centred at various spatial positions $\mathbf{x}^\alpha$ and have various structural wavenumber vectors $\mathbf{k}^\alpha$.

The wave field scattered by the perturbations is then composed of waves $u^\alpha_i(\mathbf{x},t)$ scattered by individual Gabor functions:

$$\delta u_i(\mathbf{x},t) = \sum_\alpha u^\alpha_i(\mathbf{x},t) \quad .$$

Applied approximations

Short-duration broad-band wave field with a smooth frequency spectrum incident at the Gabor function, expressed in terms of the amplitude and travel time.

First-order Born approximation of each wave $u_i^\alpha(\mathbf{x}, t)$ scattered by one Gabor function.

Ray-theory approximation of the Green tensor in the Born approximation.

High-frequency approximation of spatial derivatives of both the incident wave and the Green tensor. In this high-frequency approximation, we neglect the derivatives of the amplitude, which are of order $1/\mathit{frequency}$ with respect to the derivatives of the travel time.

Paraxial ray approximation of the incident wave in the vicinity of central point $\mathbf{x}^\alpha$ of the Gabor function.

Two-point paraxial ray approximation of the Green tensor at point $\mathbf{x}^\alpha$ and at the receiver. The paraxial ray approximation consists in a constant amplitude and in the second-order Taylor expansion of the travel time.

Initial slowness vector of the Gaussian sensitivity beam

Inverse frequency:

$$\varpi = \omega^{-1} \quad .$$

For each inverse frequency, the amplitude of the sensitivity beam depends on the distance of point $P_i + \varpi\, k_i^\alpha$ from the wavenumber surface.

Maximum amplitude of the sensitivity beam:

$$\det\{c_{ijkl}(\mathbf{x}^\alpha)[P_j + \varpi^0 k_j^\alpha][P_l + \varpi^0 k_l^\alpha] - \varrho(\mathbf{x}^\alpha)\delta_{ik}\} = 0 \quad .$$

For positive real–valued solutions ϖ^0, the initial slowness vector of the reference ray is

$$p_i^0 = P_i + \varpi^0\, k_i^\alpha \quad .$$

Inverse frequencies ϖ^0 for different structural wavenumber vectors k_i^α

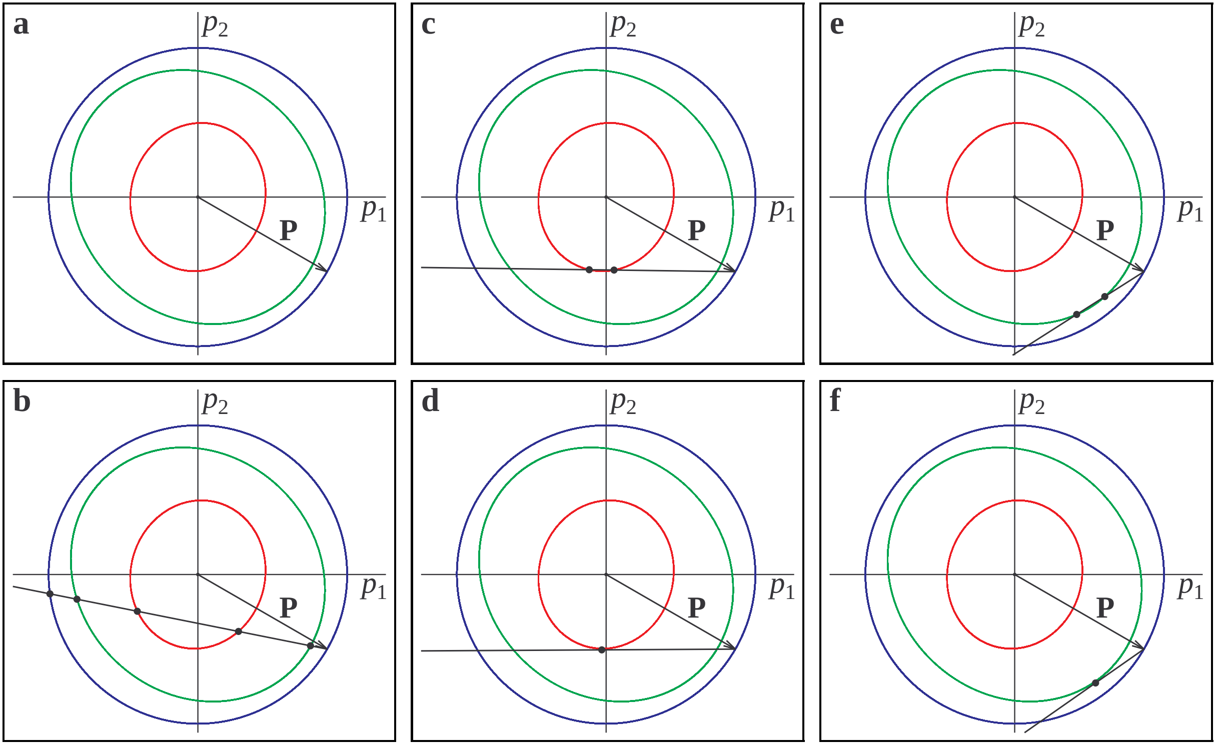

Initial slowness vector of the broad-band sensitivity beam

For close positive real–valued solutions ϖ^{01} and ϖ^{02} or for close imaginary solutions ϖ^{01} and ϖ^{02} with equal positive real parts:

$$\varpi^0 = \tfrac{1}{2}\left(\varpi^{01} + \varpi^{02}\right) \quad ,$$

$$p_i^0 = (1 - \delta p^0)^{-1}[P_i + \varpi^0\, k_i^\alpha] \quad .$$

Standard second-order paraxial approximation of the slowness vector leading to point $\mathbf{x}$:

$$p_i(\mathbf{x}) \approx p_i^0 - \tau^{0\prime}_{,ji}\Delta x_j \quad .$$

Direction-dependent relative length correction slowness vector:

$$p_i(\mathbf{x}) \simeq p_i^0 - \tau^{0\prime}_{,mi}\Delta x_m + p_i^0\,[\delta p(\Delta\mathbf{x}) - \delta p^0] \quad .$$

Paraxial approximation of the sensitivity beam in ray-centred coordinates

Paraxial approximation at frequency ω^0:

$$T^{\alpha}_{\omega^0}(\mathbf{x}) \approx T^{\alpha} + \tau^0 + \frac{\mathrm{d}\tau}{\mathrm{d}q_3}\Delta x_3^{(q)} + \frac{1}{2}\Delta x_i^{(q)} M_{ij}\Delta x_j^{(q)}$$

$$+\Delta x_K^{(q)} N_K \delta p(\Delta\mathbf{x}) + \frac{1}{2} N \left[\delta p(\Delta\mathbf{x})\right]^2 \quad .$$

Frequency dependence of the paraxial approximation :

$$T^{\alpha}_{\omega}(\mathbf{x}) \approx T^{\alpha}_{\omega^0}(\mathbf{x}) + \Delta x_K^{(q)} M_{K4}\frac{\Delta\omega}{\omega} + \frac{1}{2} M_{44}\left(\frac{\Delta\omega}{\omega}\right)^2 + N_4 \delta p(\Delta\mathbf{x})\frac{\Delta\omega}{\omega} \quad .$$

Evolution equations of the sensitivity beam

$$\mathbf{M} = \mathbf{P}\mathbf{Q}^{-1} \quad ,$$

$$\mathbf{M}_4 = {\mathbf{Q}^{-1}}^{\mathrm{T}} \mathbf{M}_4^{\alpha} \quad ,$$

$$M_{44} = M_{44}^{\alpha} - {\mathbf{M}_4^{\alpha}}^{\mathrm{T}} \mathbf{Q}^{-1} \mathbf{Q}_2 \mathbf{M}_4^{\alpha} \quad ,$$

$$\mathbf{N} = {\mathbf{Q}^{-1}}^{\mathrm{T}} \mathbf{N}^{\alpha} \quad ,$$

$$N = N^{\alpha} - {\mathbf{N}^{\alpha}}^{\mathrm{T}} \mathbf{Q}^{-1} \mathbf{Q}_2 \mathbf{N}^{\alpha} \quad ,$$

$$N_4 = N_4^{\alpha} - {\mathbf{M}_4^{\alpha}}^{\mathrm{T}} \mathbf{Q}^{-1} \mathbf{Q}_2 \mathbf{N}^{\alpha} \quad .$$

Paraxial approximation of the sensitivity packet in ray-centred coordinates

$$T^{\alpha}_{\mathbf{GP}}(\mathbf{x},t) \approx T^{\alpha} + \tau^{0} - t + \frac{\mathrm{d}\tau}{\mathrm{d}q_3}\Delta x_3^{(q)} + \frac{1}{2}\Delta x_i^{(q)} M_{\mathbf{GP}\,ij}\Delta x_j^{(q)}$$

$$+\Delta x_i^{(q)} N_{\mathbf{GP}\,i}\delta p(\Delta\mathbf{x}) + \frac{1}{2} N_{\mathbf{GP}}\left[\delta p(\Delta\mathbf{x})\right]^2$$

$$+\left[\Delta x_i^{(q)} M_{\mathbf{GP}\,i4} + N_{\mathbf{GP}\,4}\delta p(\Delta\mathbf{x})\right](t - T^{\alpha} - \tau^{0}) + \frac{1}{2} M_{\mathbf{GP}\,44}(t - T^{\alpha} - \tau^{0})^2 \quad .$$

Evolution equations of the sensitivity packet

$$M_{\mathbf{GP}\,KL} = M_{KL} - M_{K4}M_{L4}/M_{44} \quad ,$$

$$M_{\mathbf{GP}\,K4} = M_{K4}/M_{44} \quad ,$$

$$M_{\mathbf{GP}\,44} = -1/M_{44} \quad ,$$

$$M_{\mathbf{GP}\,34} = -M_{\mathbf{GP}\,44}\frac{\mathrm{d}\tau}{\mathrm{d}q_3} \quad ,$$

$$M_{\mathbf{GP}\,i3} = -M_{\mathbf{GP}\,i4}\frac{\mathrm{d}\tau}{\mathrm{d}q_3} + M_{i3} \quad ,$$

Difference from Gaussian sensitivity packets:
M_{44} may be small or zero at the initial point and at caustics.

$$N_{\mathbf{GP}\,K} = N_K - M_{K4}N_4/M_{44} \quad ,$$

$$N_{\mathbf{GP}} = N - (N_4)^2/M_{44} \quad ,$$

$$N_{\mathbf{GP}\,4} = N_4/M_{44} \quad ,$$

$$N_{\mathbf{GP}\,3} = -N_{\mathbf{GP}\,4}\frac{\mathrm{d}\tau}{\mathrm{d}q_3} \quad .$$

Illustrations of the broad-band sensitivity packets

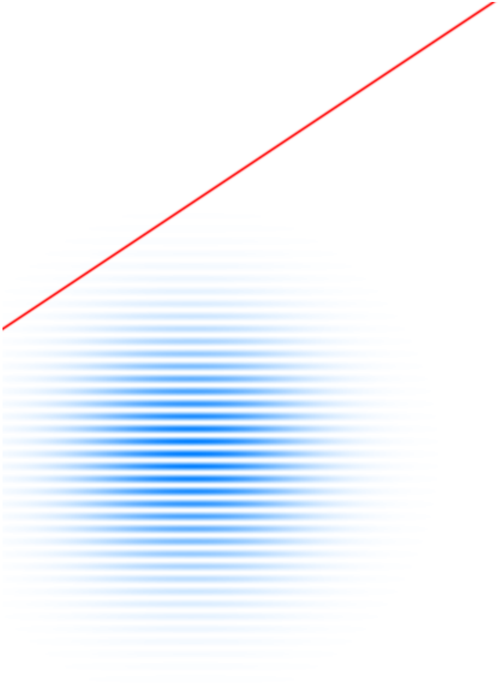

$\delta p^0 = 0.11$

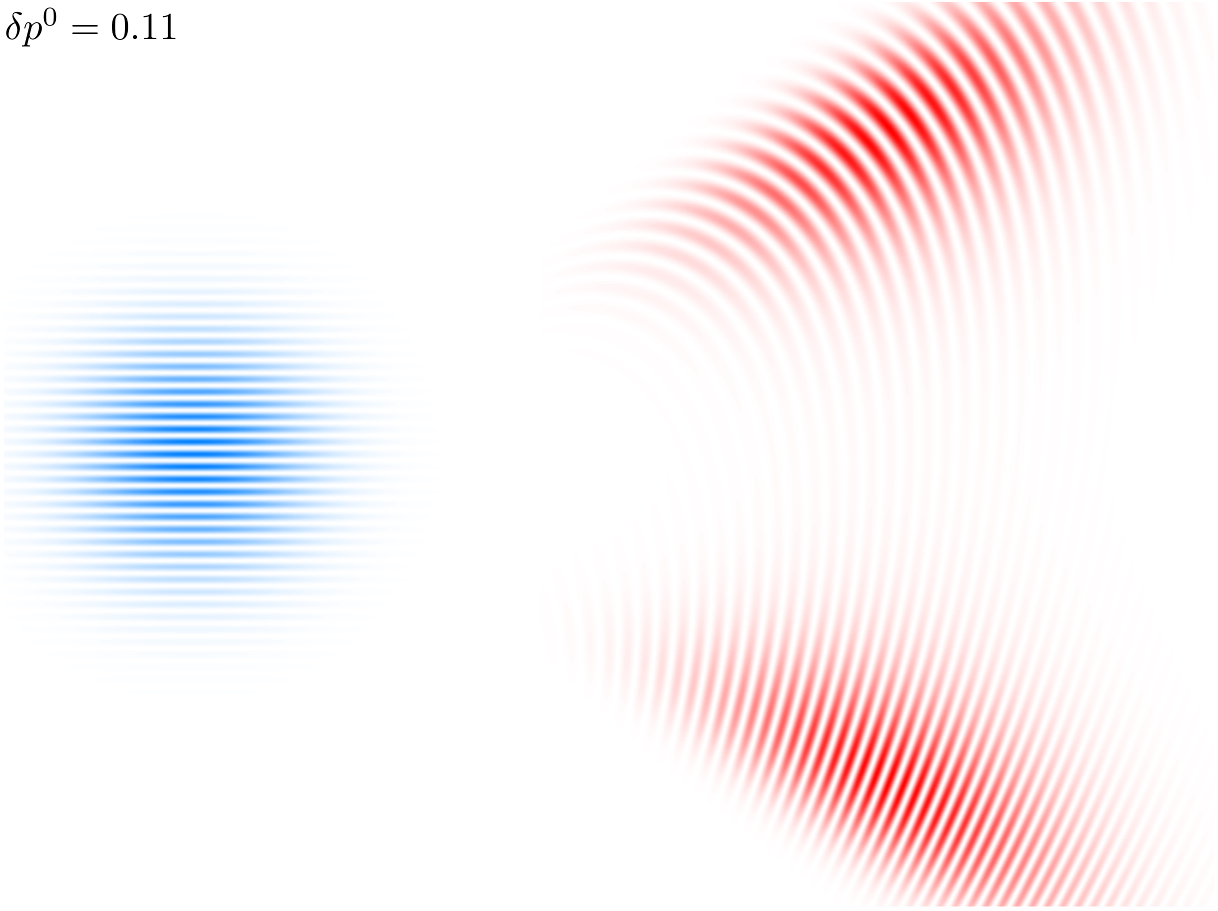

$\delta p^0 = 0.10$

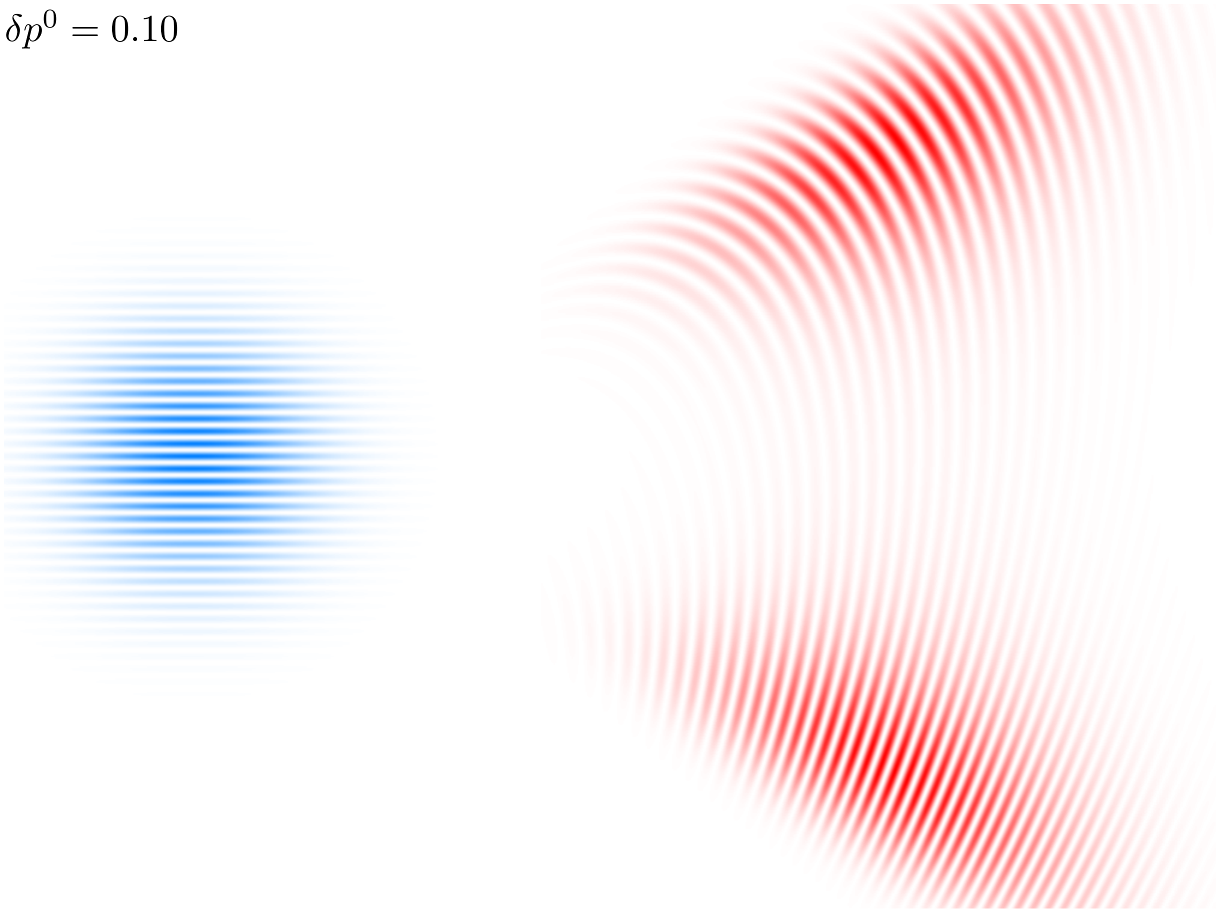

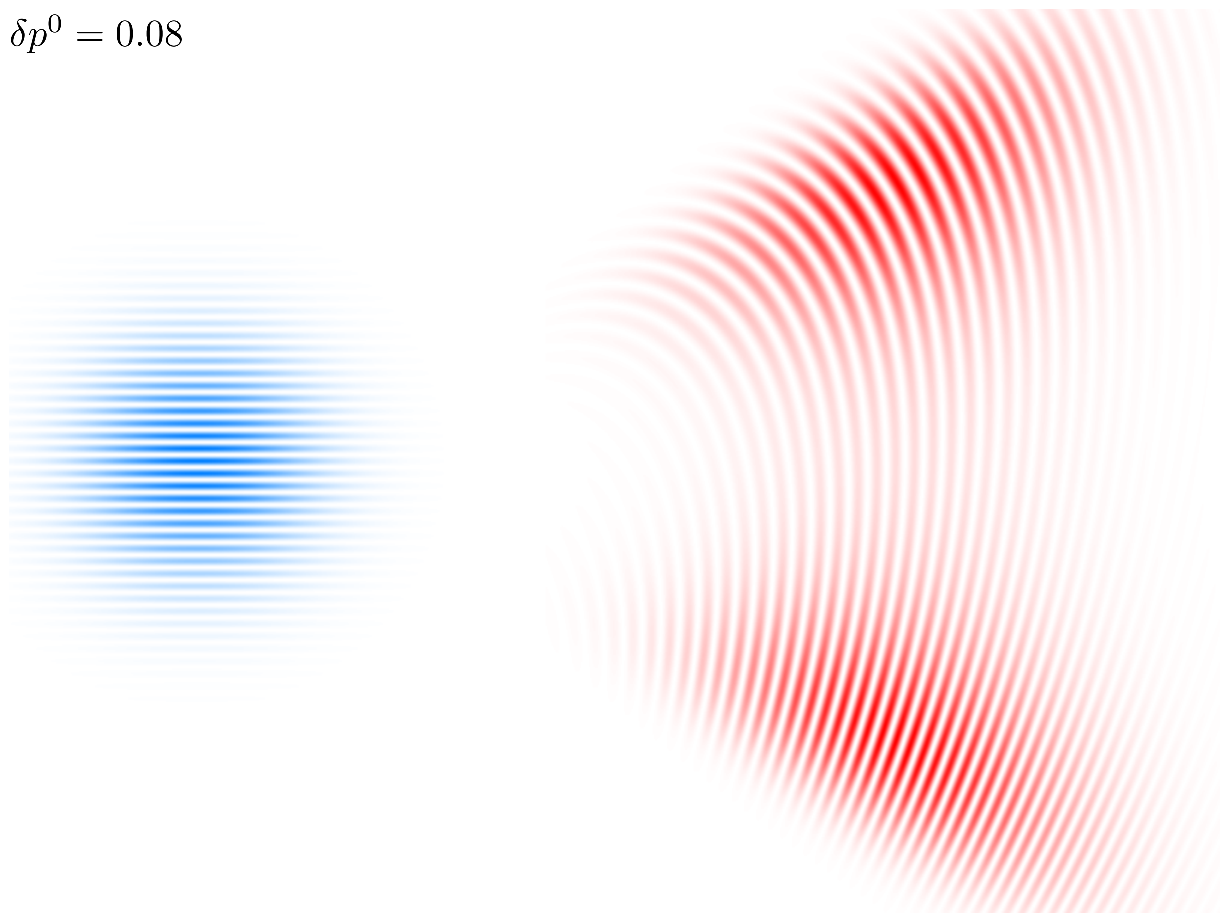
$\delta p^0 = 0.08$

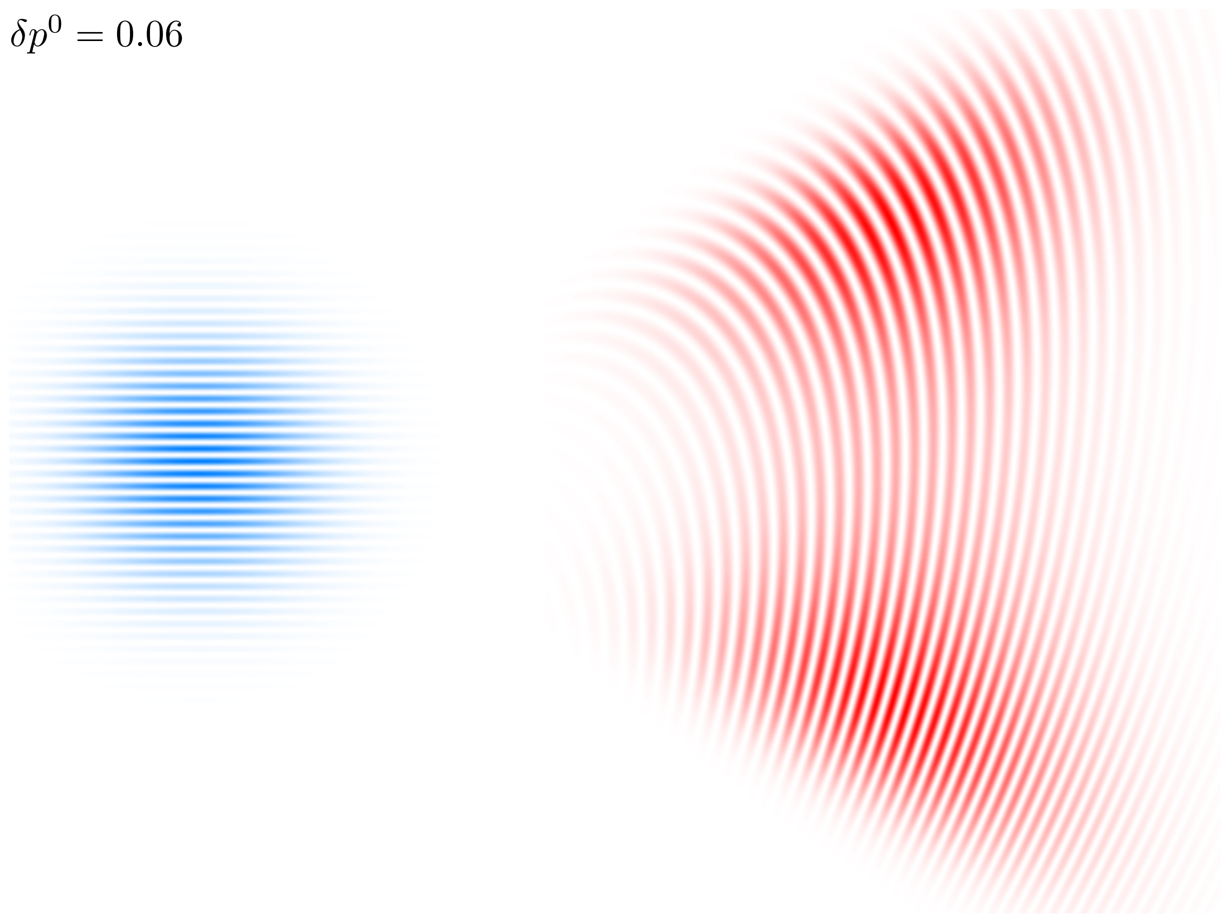
$\delta p^0 = 0.06$

$\delta p^0 = 0.04$

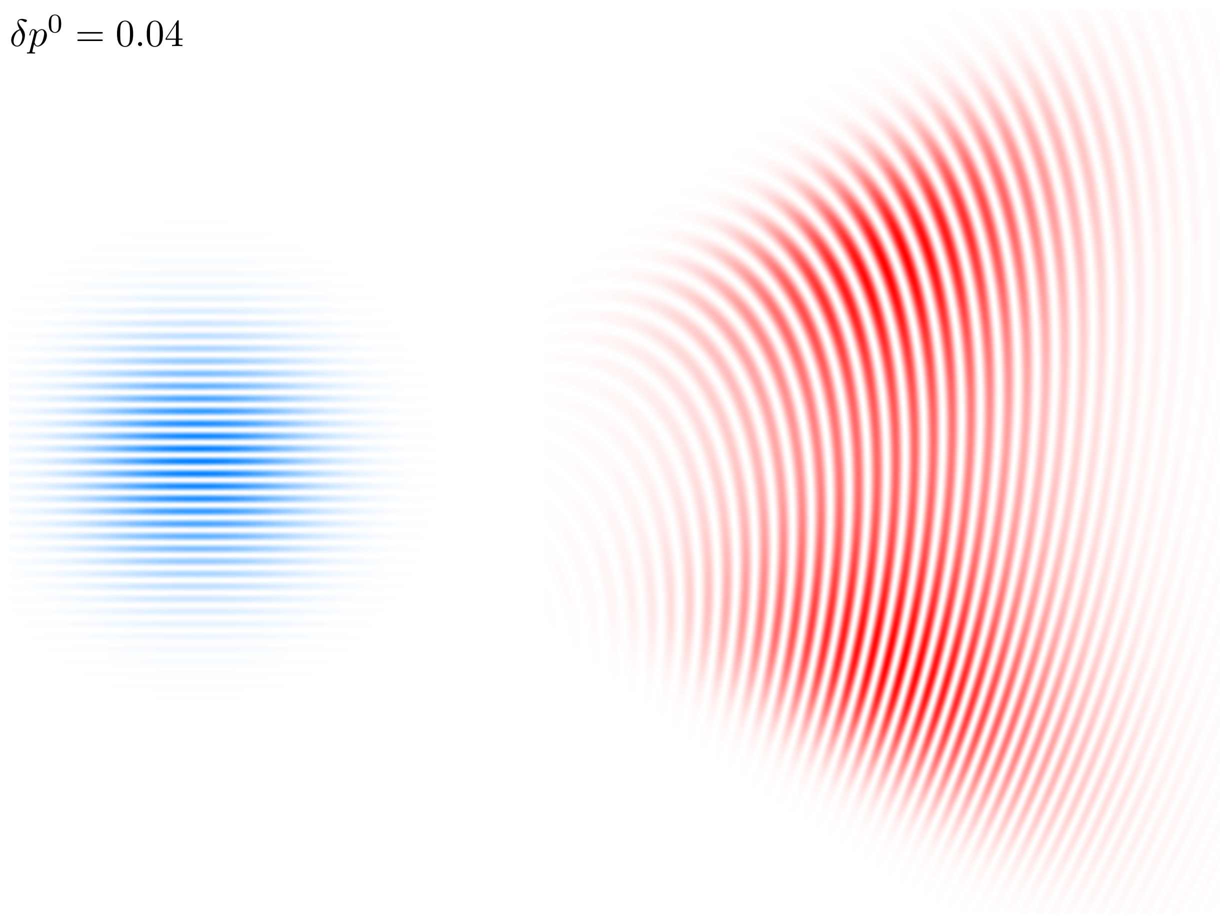

$\delta p^0 = 0.02$

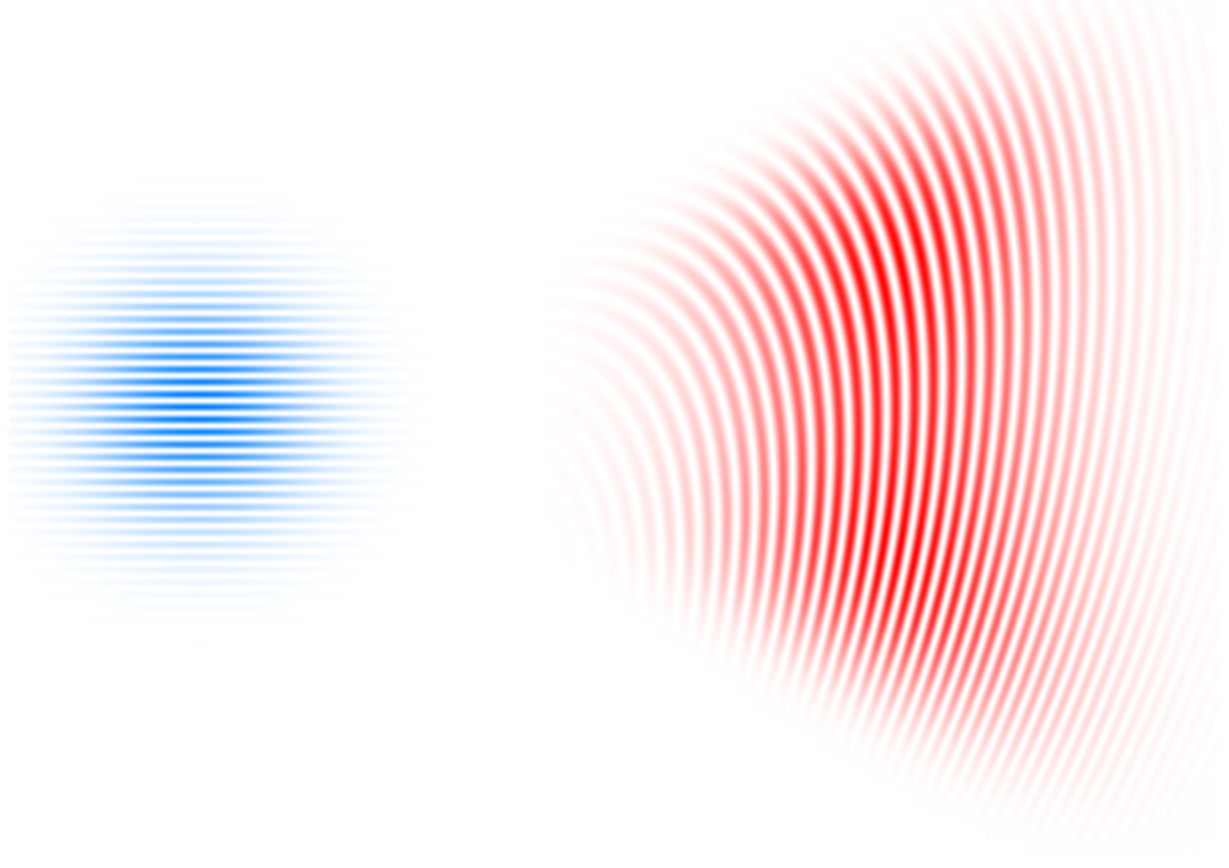

$\delta p^0 = 0.00$

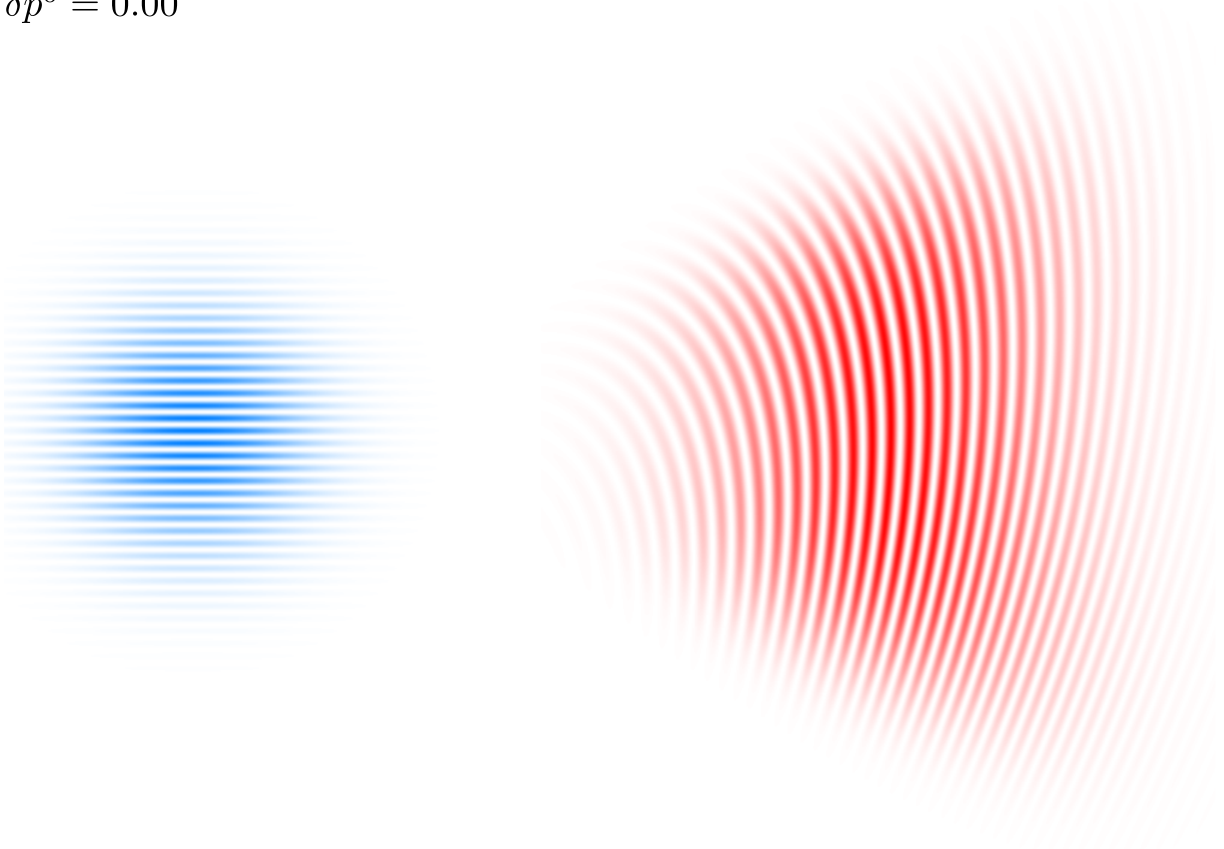

$\delta p^0 = -0.02$

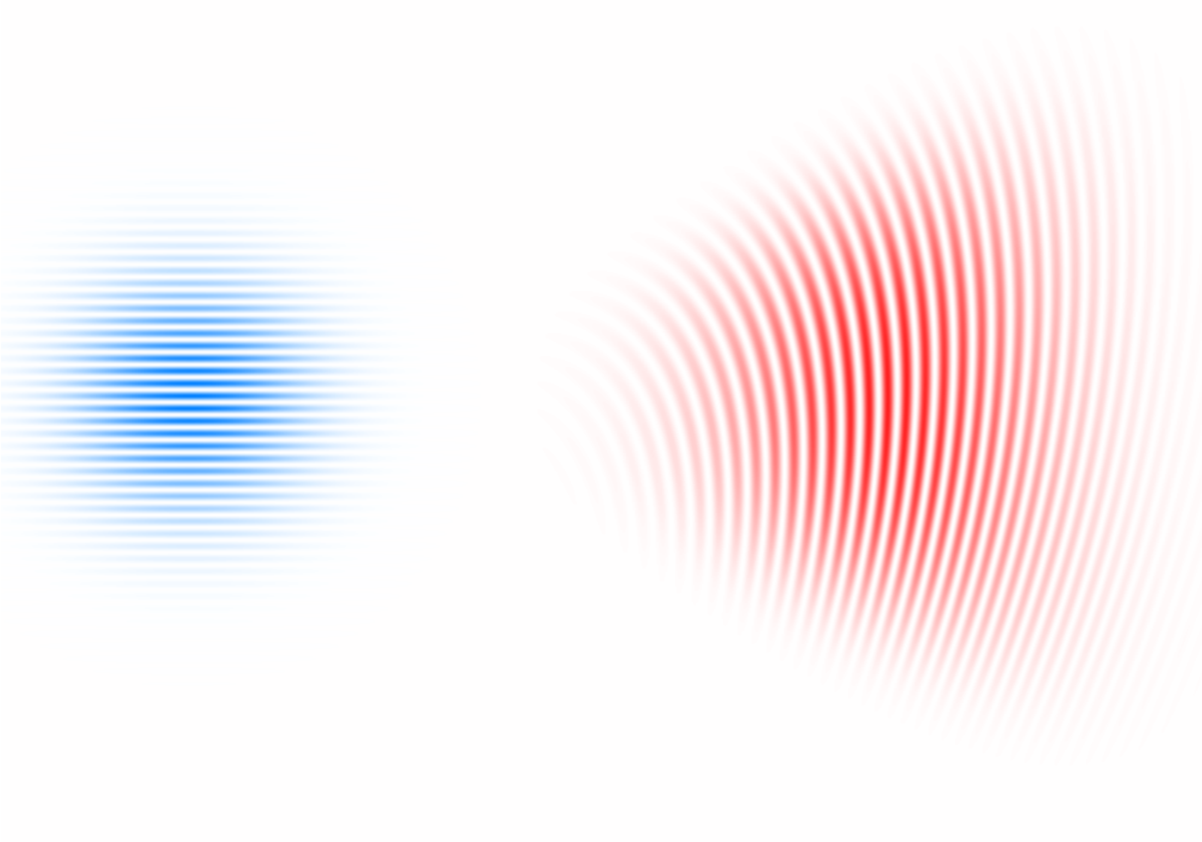

$\delta p^0 = -0.04$

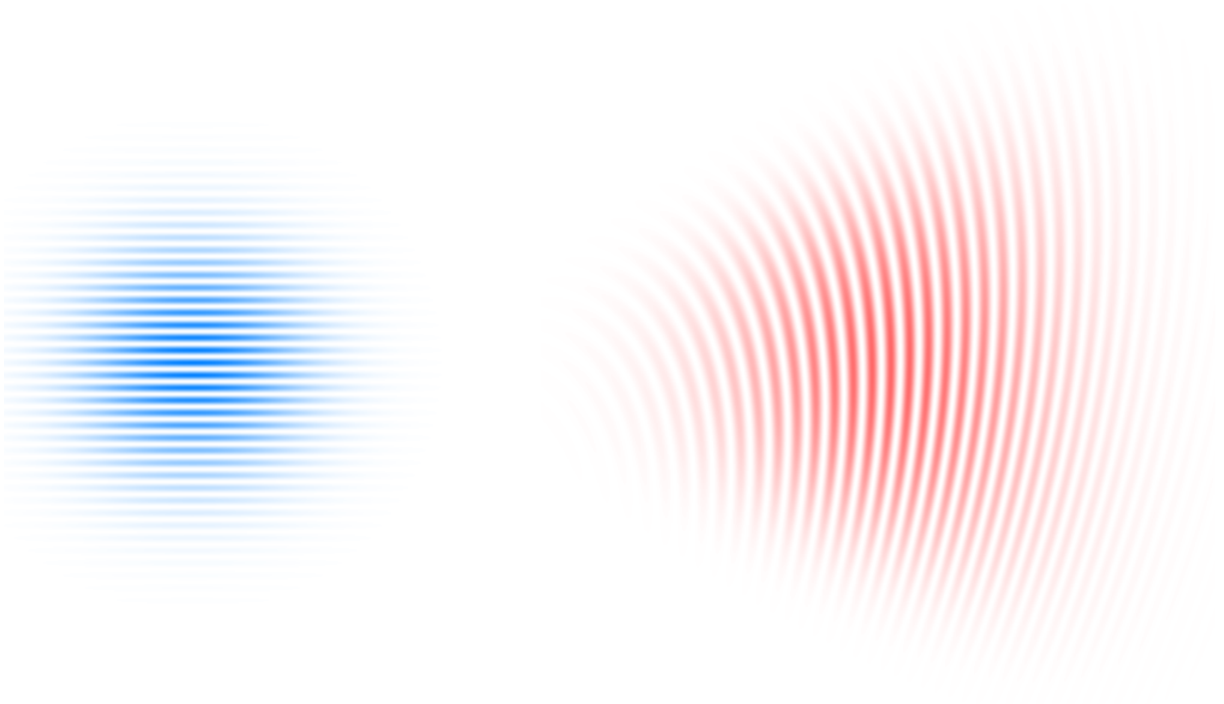

$\delta p^0 = -0.06$

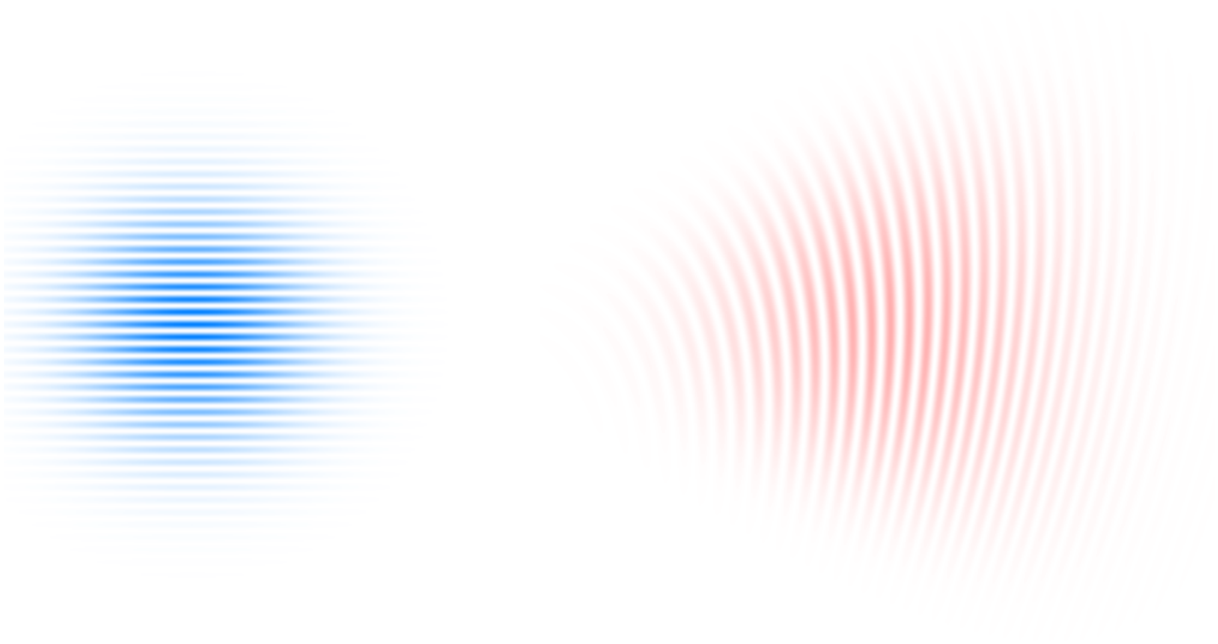

$\delta p^0 = -0.08$

$\delta p^0 = -0.10$

Conclusions

Perturbations of elastic moduli and density can be decomposed into Gabor functions.

A short-duration broad-band wave with a nearly constant frequency spectrum incident at each Gabor function generates at most 5 scattered sensitivity packets.

We have generalized the theory of narrow-band Gaussian sensitivity packets by Klimeš (2012) to wide-angle broad-band sensitivity packets.

The derived correspondence between the perturbations of the structure and the recorded wavefield may play a decisive role in understanding the information on geological structures carried by seismic wavefields, in understanding the physical meaning of velocity models, and in interpreting seismic data from forward to wide–angle scattering. It may help us in designing the optimum target–oriented reflection measurement configuration, see Klimeš (2010).

References (online at "http://sw3d.cz")

Klimeš, L. (2010): Sensitivity Gaussian packets. In: *Seismic Waves in Complex 3-D Structures, Report 20*, pp. 29–34, Dep. Geophys., Charles Univ., Prague.

Klimeš, L. (2012): Sensitivity of seismic waves to structure. *Stud. geophys. geod.*, **56**, 483–520.

Klimeš, L. (2013): Sensitivity of seismic waves to structure: Wide-angle broad-band sensitivity packets. In: *Seismic Waves in Complex 3-D Structures, Report 22*, pp. 17–44, Dep. Geophys., Charles Univ., Prague.

Acknowledgements

The research has been supported:

by the Grant Agency of the Czech Republic under contract P210/10/0736,

by the Ministry of Education of the Czech Republic within research project MSM0021620860,

and by the consortium “Seismic Waves in Complex 3-D Structures”

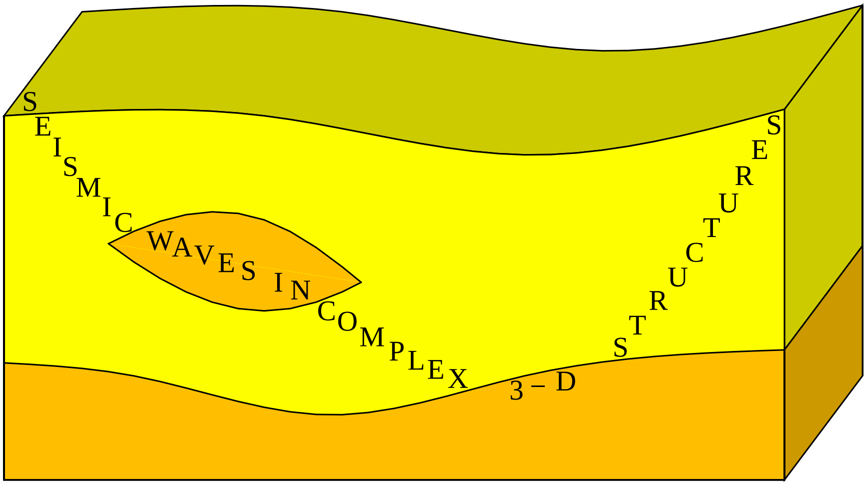

http://sw3d.cz